Continental Shelf Research 148 (2017) 44–52

Contents lists available at ScienceDirect

Continental Shelf Research

journal homepage: www.elsevier.com/locate/csr

Analysis of tidal amplitude changes using the EMD method

Yongcun Cheng[a,b], Tal Ezer[a], Larry P. Atkinson[a], Qing Xu[c,*]

[a] Center for Coastal Physical Oceanography, Old Dominion University, Norfolk, VA, USA
[b] Beijing Piesat Information Technology Co. Ltd., Beijing, China
[c] College of Oceanography, Hohai University, Nanjing, China

ARTICLE INFO

Keywords:
Tide
EMD
Harmonic analysis
Sea level

ABSTRACT

Empirical Mode Decomposition (EMD) analysis of sea level data has been used in the past mostly to study long-term sea level rise (SLR) and decadal/multidecadal variations. However, application of EMD to high-frequency sea level variability is rare, so here EMD is tested as a tool to analyze hourly sea level data and detect time-dependent changes in tidal characteristics. Traditional Harmonic Analysis (HA) cannot deal with non-linear, non-stationary processes such as storm surges. Here, the two methods are compared in the analysis of 17 tide gauge records from the U.S. East Coast, demonstrating considerable trends and interannual variability in the semidiurnal tides. The time dependent changes of tidal characteristics are unique for each region and in some cases for specific locations. The results show that in most stations the highest and second-highest frequency modes of the EMD can capture the semidiurnal and diurnal tides, respectively. High correlation is often found between the variations of the first EMD mode and the amplitude of the M_2 tide obtained from HA. However, in some locations the high frequency EMD mode captures other (non M_2) variability and in other locations a sudden shift in tidal characteristics is found. In Baltimore for example, during the 1970s the amplitude suddenly increased for the M_2 tide but decreased for the S_2 tide, and in Wilmington a significant increase (~ 20 cm in ~ 80 years) in the amplitude of the M_2 tide is detected by both methods. These changes could indicate an instrumental change or a morphological change due to storm surges. This short report is meant to demonstrate a new tidal analysis tool that can help studies of changes in tidal characteristics and the relation of these changes to morphology change, sea level rise and climate change.

1. Introduction

The U.S. Northeastern coast has been identified as a ‘hotspot’ of accelerated sea level rise (SLR, Ezer and Corlett, 2012; Sallenger et al., 2012) and accelerated flooding (Ezer and Atkinson, 2014). The region shows a significantly higher SLR trend than global mean SLR (Church and White, 2011; Houston and Dean, 2011). This is due to a combination of land subsidence and potential slowdown of the Atlantic Meridional Overturning Circulation (AMOC) and a weakening of the Gulf Stream (GS) flow (Ezer, 2015; Ezer et al., 2013). Over time, SLR increases the damage to low-lying coastal communities during storm surges (Tebaldi et al., 2012; Wahl et al., 2014; Wahl and Chambers, 2016; Wdowinski et al., 2016) and increases the frequency of minor tidal flooding (Sweet and Park, 2014). Since minor flooding is related to the combination of SLR and tidal amplitude (Ezer and Atkinson, 2014), it is important to detect any changes in the characteristics of tides over time. Note however, that tidal amplitude itself can also be affected by SLR (e.g., Pickering et al., 2017).

Recent studies have found an increase in the M_2 tidal amplitude in the Gulf of Maine (Ray, 2006, 2009) and along the U.S. East Coast (Woodworth, 2010). Coherent linear trends of tidal range in the last 30–90 years have been reported over the regions (Flick et al., 2003). Müller (2011) pointed out that the physical causes of tide trends and their spatial variability are uncertain and it is difficult to relate them to other oceanic or atmospheric variables, though there are evidences that SLR can affect tides in coastal regions (Pelling et al., 2013). Numerical modeling experiments of the impact of future SLR on tides demonstrate a complex response, so that for the same SLR rate, tidal energy may increase on one coast and decrease in another nearby coast (Lee et al., 2017). Although the land motion due to Glacial Isostatic Adjustment (GIA) and SLR contribute to the trend of tidal amplitudes, numerical simulations have difficulties to reproduce the spatial pattern of the tidal trend (Müller, 2011), since the complicated mechanisms of tidal characteristic changes (Mawdsley et al., 2015). Therefore, changes in tidal characteristics due to SLR and other climatic changes can be very different between one region and another (Woodworth, 2010; Pickering

* Corresponding author.
E-mail address: xuqing0215@hotmail.com (Q. Xu).

http://dx.doi.org/10.1016/j.csr.2017.09.009
Received 11 January 2017; Received in revised form 11 September 2017; Accepted 21 September 2017
Available online 23 September 2017

et al., 2017).

This study was motivated by the need to better detect changes in the variability of tides which, when combined with uncertainty in SLR, can increase risk of flooding (Greenberg et al., 2012). Low-lying populated regions such as the Hampton Roads in Virginia, Miami Beach in south Florida, and Boston are examples of areas that are especially vulnerable flooding due to SLR (Atkinson et al., 2012; Ray and Foster, 2016; Wdowinski et al., 2016; Zhang, 2011; Zhang and Sheng, 2013).

The common method used to study the changes in tides is harmonic analysis (HA, (Foreman, 1977)), which can be applied for example to hourly sea level records obtained from tide gauges. This work aims to test the feasibility of using Empirical Mode Decomposition (EMD) analysis (Huang et al., 1998; Huang and Wu, 2008) to detect changes in the semidiurnal tide amplitude. This new tidal analysis method could supplement the standard HA. The EMD method is a non-stationary and nonlinear time series analysis method, so that irregular patterns of storm surges, or tidal amplitude changes over time are good test cases for this method. The method decomposes any time series data into a finite number of intrinsic mode functions (oscillating modes) with time-variable amplitudes and frequencies, plus a residual (or trend). EMD has been widely used for analysis of different geophysical data (Wu and Huang, 2009), as well as for other applications such as in seismic, medical and economic data.

In recent years, applications of the EMD method for analysis of sea level data have focused on calculations of SLR trends, SLR acceleration and long-term sea level variability (e.g., Ezer and Corlett, 2012; Bonaduce et al., 2016; Cheng et al., 2016; Ezer, 2013, 2015; Ezer et al., 2016; F. Li et al., 2016; Y. Li et al., 2016), sea level reconstruction (e.g., Sha et al., 2015) and future SLR projections. Note that in the above studies the EMD was used to filter out high-frequency oscillations to discover lower-frequency variations, while here the high-frequency oscillations are the main subject of the research. Therefore, in this new application the EMD is used to analyze high-frequency modes to test if they can describe the variability of the M_2 and other semidiurnal tides (M_2 is the dominant constituent of tides along the U.S. East Coast). Note that because EMD is a non-stationary method, it can detect time-dependent changes in amplitude and frequency with one calculation of an entire record, while the HA will require multiple calculations, each one using small sub-sections of the data (say 1 year) to see if the tidal characteristics change over time. On the other hand, the disadvantage of the EMD is that it is a non-parametric method (frequencies are not specified and oscillations are not assumed to be sinusoidal) and thus it cannot guarantee to extract the known tidal constituents. Therefore, the proposed EMD analysis needs to be tested against standard methods to learn of its usefulness and limitations.

The paper is organized as follows. The tide gauge sea level records and the methodology employed in this study are described in Section 2. The results are presented in Section 3 and the discussion and summary are provided in Section 4.

2. Dataset and methodology

2.1. Tide gauge sea level records

Hourly tide gauge data were obtained from NOAA (http://opendap.co-ops.nos.noaa.gov/dods/). Fig. 1 shows the locations of the selected 17 tide gauges along the U.S. coast. Most stations provide long and continuous sea level records (average starting year ~1917; see Table 1) except 2 stations in the lower Chesapeake Bay starting in the 1970s' (No. 10 and 11). The 2 shorter records are located in a region with significant land subsidence (Kopp, 2013). Our study includes more stations than a previous study of the issue (Müller, 2011).

2.2. Harmonic analysis

The standard tool for tidal analysis is often based on HA. Available

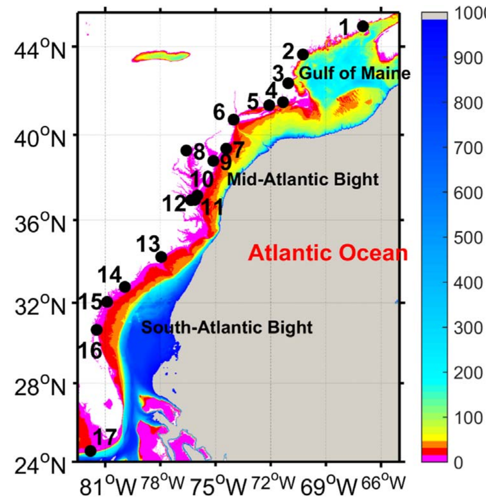

Fig. 1. Bathymetry of the study area and location of the selected tide gauges (the numbers according to the tide gauges listed in Table 1). The regions with water depth larger than 1000 m are marked as grey.

software includes for example, TASK (Tidal Analysis Software Kit, Bell et al., 1996), T-tide (Pawlowicz et al., 2002) and Utide (Codiga, 2011). The Utide was selected to calculate all tidal constituents for its capability in solving the nodal cycle with the default settings. Experiments (not shown) with subset windows of 1, 2 or 3 years show very little effect on the results. The HA is applied to hourly data in each year. Then the results of all years provide a time series of the M_2 tidal amplitude which then is compare with that computed from the EMD method (see below).

2.3. Empirical mode decomposition

To detect changes in tidal amplitudes, we analyze the high frequency modes obtained for each station using EMD. The EMD of a sea level record from location M would be represented by

$$h^M(t) = \sum_{i=1}^{N} c_i^M(t) + r^M(t) \tag{1}$$

where N denotes a finite number of oscillating modes, c_i *(t)* is intrinsic oscillatory modes, and *r(t)* is a residual (or "trend"). The number of modes depends on the record length and the amount of variability. The oscillating modes are calculated by a repeated sifting process (a kind of filter) until only the residual is left. A Hilbert spectrum transform is applied for each mode to provide a time-dependent estimation of the frequency of the oscillations (thus EMD is often called a Hilbert-Huang Transform, HHT; Huang et al., 1998). Note that particular modes do not necessarily represent specific processes, but the analysis allows the separation of noisy records into oscillations with different time scales. Statistical confidence levels for EMD modes can be calculated using variations in the sifting parameters (Huang et al., 2003), bootstrap methods (Ezer and Corlett, 2012) or ensemble with white noise simulations (Ezer, 2016). However, no quantitative examination of each mode is done here, only the 1-year average magnitude of the peaks of the highest frequency EMD mode is examined, to test if it is consistent with changed in the dominate M_2 tidal constituent obtained by the HA. More detailed statistical examination is left for future follow up studies. Appendix Fig. A1 shows an example of the 19 EMD modes for station Baltimore (for discussion of the interannual and decadal variability in this and other sea level records, see previous studies such as Ezer (2013, 2015).

For consistency purposes, both the EMD analysis and HA adopt the least-square fitting method in Müller (2011) to determine the linear trend (A). To remove the long-term nodal cycle (amplitude A_N; period

Table 1
Details of the selected Hourly Sea-Level Data (CBBT: Chesapeake Bay Bridge Tunnel, Norfolk: Sewells Point). Shown for each site are the station location (Latitude °N, Longitude °W) starting year (end in 2016), and comparisons of the mean M_2 tide amplitude (HA Amp., m) with the mean amplitude of EMD mode-1 (after removal of the nodal cycle, m). Also shown are the correlation coefficient between HA and EMD (Fig. 3) and the mean periods (hours) of the EMD modes 1 and 2.

Name (State)	Lat. (°)	Long. (°)	Start year	HA Amp.	EMD	Correlation (r)	Periods (Mode 1/2)
1. Eastport, ME	44.90	−66.98	1929	2.64	2.75	0.94	13.01/24.23
2. Portland, ME	43.66	−70.25	1910	1.35	1.36	0.93	12.62/24.29
3. Boston, MA	42.36	−71.05	1921	1.37	1.43	0.81	13.06/24.17
4. Newport, RI	41.51	−71.33	1930	0.51	0.49	0.01	5.89/22.34
5. New London, CT	41.36	−72.09	1938	0.36	0.37	0.66	12.89/23.64
6. Battery, NY	40.70	−74.01	1920	0.66	0.67	0.89	12.95/23.76
7. Atlantic City, NJ	39.36	−74.42	1911	0.58	0.59`	0.30	12.82/23.30
8. Baltimore, MD	39.27	−76.58	1902	0.15	0.11	0.82	10.78/17.61
9. Lewes, DE	38.78	−75.12	1919	0.60	0.61	0.76	12.75/24.09
10. Kiptopeke, VA	37.17	−75.99	1976	0.39	0.39	0.63	12.56/23.94
11. CBBT, VA	36.97	−76.11	1975	0.38	0.38	0.60	12.45/25.56
12. Norfolk, VA	36.95	−76.33	1927	0.36	0.36	0.41	12.56/23.96
13. Wilmington, NC	34.23	−77.95	1908	0.58	0.61	1.00	12.97/24.34
14. Charleston, SC	32.78	−79.93	1899	0.77	0.78	0.90	12.72/24.13
15. Fort Pulaski, GA	32.04	−80.90	1935	1.01	1.04	0.79	12.82/24.25
16. Fernandina, WL	30.67	−81.47	1898	0.88	0.90	0.90	12.80/24.28
17. Key West, FL	24.56	−81.81	1913	0.17	0.15	0.58	11.98/20.02

~ 18.6 years) from the EMD, the following widely used (Woodworth, 2011) relation was used:

$$\xi(t) = A_0 + At + A_N sin\left(\frac{2\pi}{18.5996}(t-1973.66)\right) + A_N cos\left(\frac{2\pi}{18.5996}(t-1973.66)\right) \quad (2)$$

Note that the nodal cycle is explicitly removed from the HA in the Utide code using a slightly different relation (but it has essentially similar purpose and result as Eq. (2)). When EMD is compared with HA, it is corrected using Eq. (2). Appendix Fig. A2 shows that even without the nodal correction of EMD the difference in tidal amplitude variation between the two methods is quite small (~ 5%, Eastport), but the remaining difference is mainly associated with the nodal cycle following Eq. (2) this demonstrates that applying the nodal correction makes the two methods much more consistent with each other.

3. Results

Previous studies show that the tide gauge stations in the study area have mostly a positive trend in the M_2 amplitude, but negative trend at Newport. The results presented below are generally consistent with

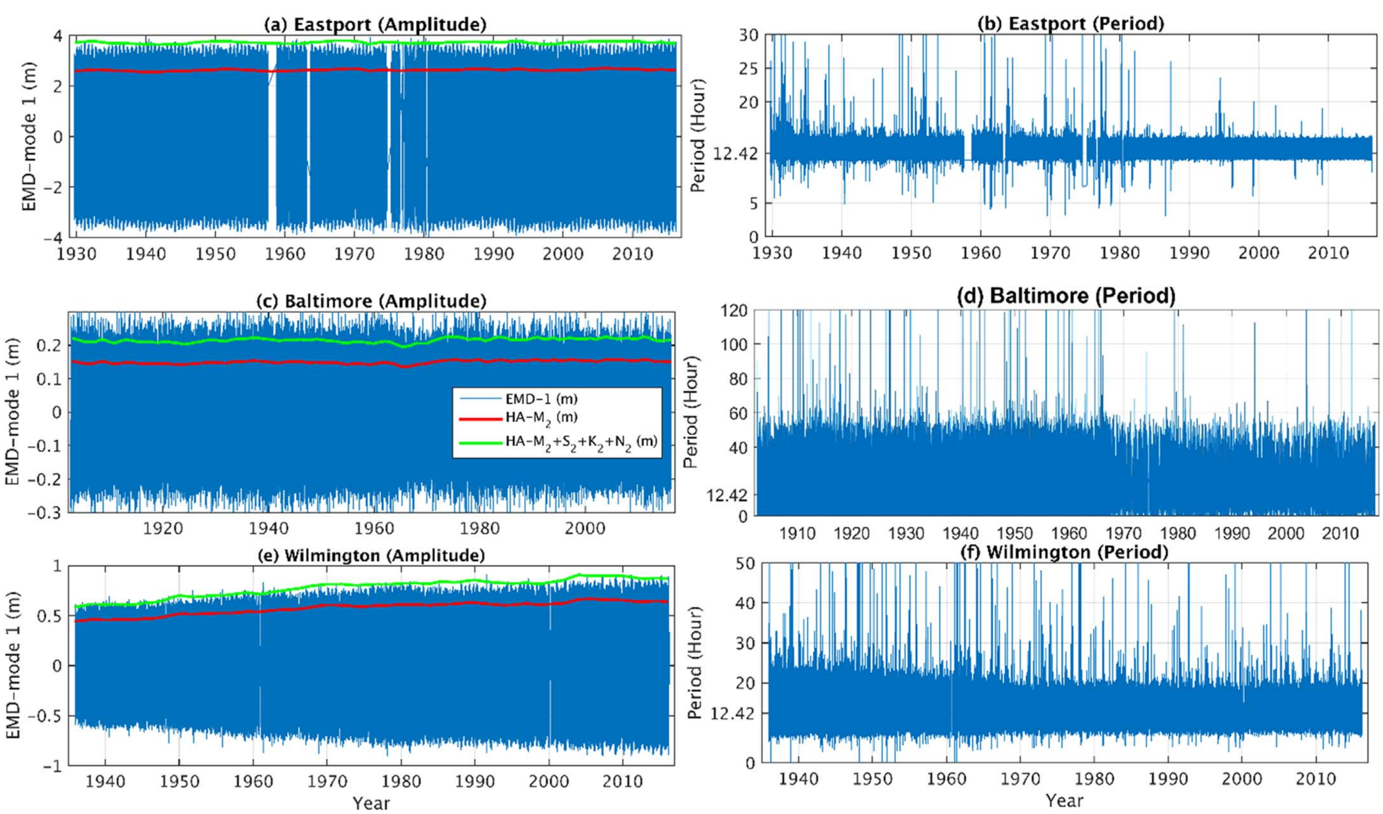

Fig. 2. Amplitude (left panels, m) and period (right panel, hours) of EMD mode-1 (blue lines) at three location (from top to bottom): Eastport (a and b), Baltimore (c and d) and Wilmington (e and f). Also shown are the annual mean amplitude of HA (from Utide, m) for the M_2 tide (red lines, m) and for the combined four semidiurnal tides (green lines, m). The period of the M_2 is indicated on the right panels. (For interpretation of the references to color in this figure legend, the reader is referred to the web version of this article.)

previous studies, but include additional locations. Negative amplitude changes at Chesapeake Bay Bridge Tunnel, Lewes and Sewells Point (Norfolk) are found by Woodworth (2010). The largest and most interesting increase in tidal amplitude occurs at Wilmington, where the tide gauge location upriver is strongly affected by sediment accumulation, as previously indicated (Ezer and Atkinson, 2014; Ray, 2009). The new EMD analysis below will shed more light on the previous reported tidal changes.

Fig. 2 demonstrates the EMD analysis (amplitude and period of oscillations) of the high frequency mode (EMD mode-1 in blue) for three stations of peculiar characteristics. In Fig. 2 (right panels), the meaningful part of the signal lies in the average frequency (or period) for each mode and potential trend in the mean, while the high frequency variations are considered as noise relative to the mean (keeping in mind that the EMD captures not only tides, but also other variations due to weather, storms, etc.). The annual mean tidal amplitudes from the HA for the M_2 tide (red lines) and combined semidiurnal tides ($M_2 + S_2 + K_2 + N_2$, green lines) are also shown. In the first station, Eastport (Gulf of Maine, Fig. 2a and b), the tidal amplitude is very large ($\sim$ 2.7 m for the M_2 tide and $\sim$ 3.8 m for all the semidiurnal tides), and semidiurnal tides other than M_2 contribute more than 1 m to the amplitude detected by the EMD. In the second station (Baltimore, MD, in the upper Chesapeake Bay; Fig. 2c and d), the tides are relatively small ($<$ 0.2 m) and the non M_2 semidiurnal tides only contribute about 0.06 m. A peculiar result is the change in frequency around 1970 (Fig. 2d), which will be further discussed later. The third station, Wilmington NC (in the Middle-Atlantic Bight; Fig. 2e and f) is chosen for its large increase in tidal amplitude due to sediment accumulation in the river in which it is located (Ezer and Atkinson, 2014). In 81 years, the amplitude of the M_2 tide increased by $\sim$0.2 m, while the amplitude of all the semidiurnal tides increased by almost 0.3 m (Fig. 2e). Interestingly enough, the EMD indicates that the frequency of mode-1 has changed as well (Fig. 2f). The later may relate to changes in the internal dynamics in the river when the morphology changed (Ray, 2009).

Table 1 summarizes the mean values of M_2 tidal amplitudes and EMD analyzed sea level magnitude (mode 1) at all sites after the nodal cycle has been removed. The M_2 tidal amplitude varies from $\sim$0.2 m (Baltimore, Key West, No 2 and 10 in Fig. 1) to $\sim$ 2.7 m (Eastport, No 8 in Fig. 1). The mean values of EMD first mode are coherent with that calculated from HA (Table 1). The mean period of EMD mode-2, generally representing the diurnal tides, is also listed in Table 1 and examples of mode-2 are shown in Appendix Fig. A3. The calculated mean periods of EMD mode 1 and 2 are consistent with the periods of semidiurnal and diurnal tides at most of the tide gauges, but there are some exceptions (see discussion below). It should be kept in mind that the EMD acts essentially as a dyadic filter (Flandrin et al., 2004), but it is not build like HA to detect particular frequencies (such as tidal constituents), so that water level variations caused by forces other than astronomical tides, such as storm surges, weather system and variations in the Gulf stream (Ezer, 2016) are captured by the EMD. The frequency calculation in EMD (or Hilbert–Huang transform; Huang et al., 1998) is a spectral method and filter performed on each mode. It can be seen as a modification of standard Fast Fourier transform or Wavelet analyses that allows to analyze non-stationary non-linear time series, providing an estimate of how the frequency for each mode changes with time. Further calculations (not shown) demonstrates that the period of mode 3 is around twice of that of mode 2. At some stations, the mean period of the oscillations in EMD mode-1 did not agree well with the period of the M_2 tide, most notably at Newport where the period of mode-1 was close to 6 h. The reason for this discrepancy is that at Newport there is a significant contribution from the M_4 tidal constituent (with a period of $\sim$ 6 h and amplitude of $\sim$ 6 cm). While in most stations the amplitude of the M_4 tide is less than 1% of the M_2 tide, in Newport it is 12%. The discrepancy of EMD-derived semidiurnal periods in Baltimore will be

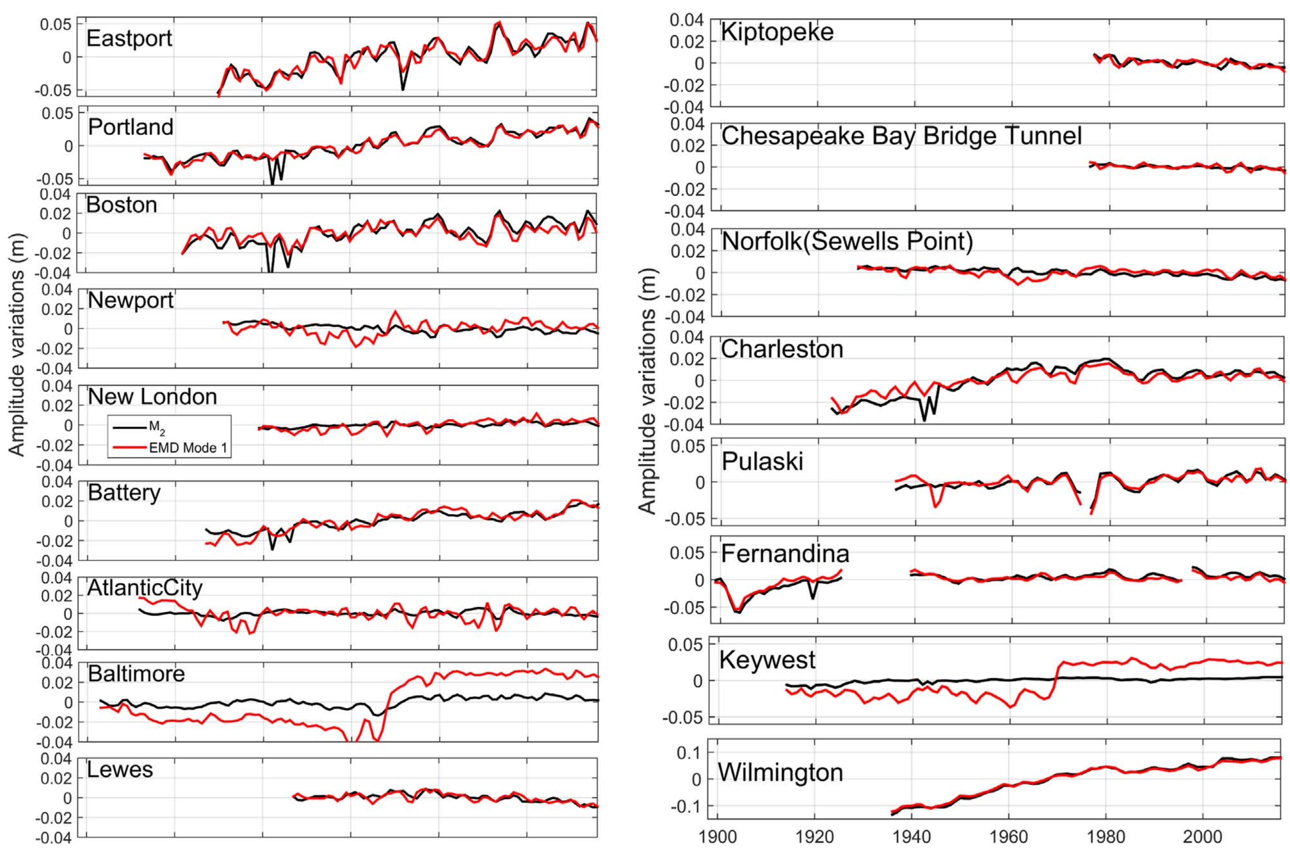

Fig. 3. Evolution of M_2 amplitude estimated using HA (black lines, m) and EMD mode-1 (red lines, m) method. The nodal cycle and the mean amplitude at each location have been removed. (For interpretation of the references to color in this figure legend, the reader is referred to the web version of this article.)

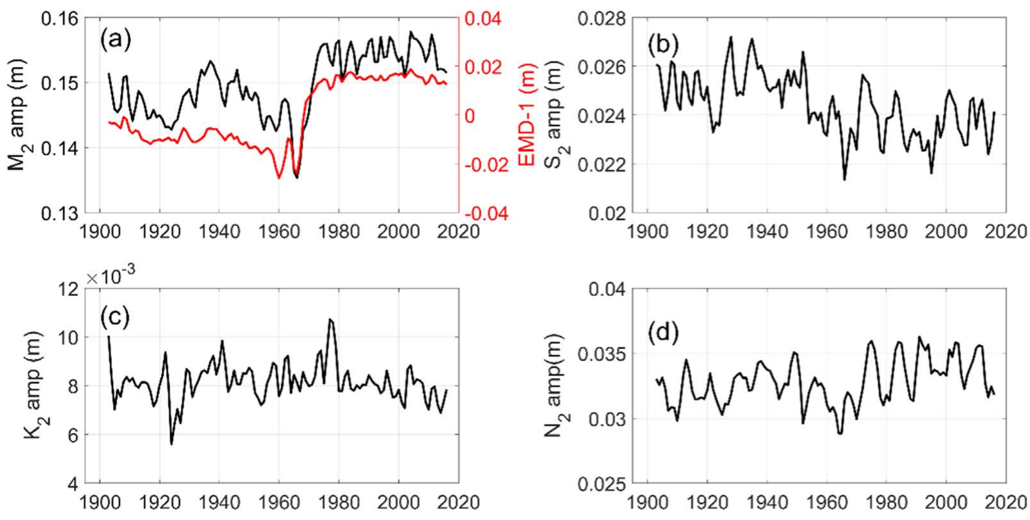

Fig. 4. Analysis of the semidiurnal tides in Baltimore obtained by HA (black lines, m): (a) M_2, (b) S_2, (c) K_2 and (d) N_2. Also shown in (a) is the amplitude of EMD mode-1 (red line. Note the different y-axis on the righ, m). (For interpretation of the references to color in this figure legend, the reader is referred to the web version of this article.)

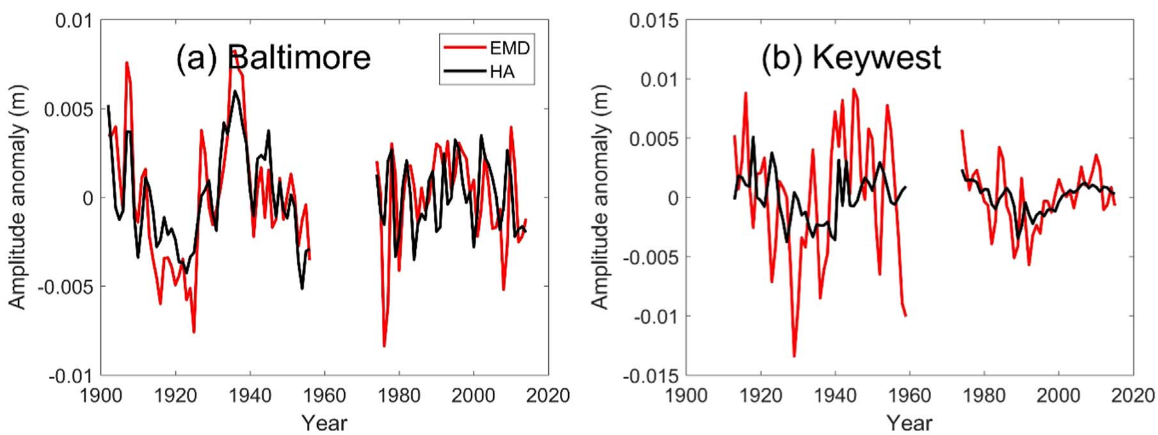

Fig. 5. Similar to Fig. 3 but for the tide gauge records when they are separated into two time series, before and after the amplitude jump around 1960; (a) Baltimore and (b) Keywest.

discussed later.

Fig. 3 compares the variations of the M_2 amplitude estimated by the HA with the variations of the amplitude of the EMD mode-1. The nodal cycle and mean values have been removed at each tide gauge and the correlation coefficients between the time series are listed in the table. The correlations are higher than 0.6 at most of the sites and reach up to ~1.0 at Wilmington (which shows the largest increase in tidal amplitude of any station). Low correlations are presented at Atlantic City and Sewells Point (Norfolk) and the lowest correlation observed at Newport. The Atlantic City station faces the open Atlantic Ocean, so that the magnitude of sea level variations in the EMD first mode maybe affected by coastal or offshore ocean circulation changes. At Norfolk, both methods show almost identical downward trend (i.e., a constant decrease in M_2 amplitude), but insignificantly small and random interannual variations which could explain the low correlation. Clear shifts in amplitude and phase of tidal constituents may attributes to small changes in tide gauge location or surrounding coastal morphology (Mawdsley et al., 2015). Both the Newport and Sewells Point are located inside rivers/harbors, so local topography seems to impact the variations of tidal constituents (Jay, 2009), and as mentioned before, the M_4 tides is nonnegligible in Newport (i.e., it is captured by the EMD, but ignored in the HA). Notes that the EMD amplitude indicates a jump at Baltimore and Key West in 1960–1970 and the EMD shows larger sea level variations than HA at these locations. There was a reported tide gauge instrument replacement in 1967 at Key West that the EMD analysis may have detected. At Pulaski, the data gaps in 1974 is also due to the tide gauge instrument change, which captured by the two approaches. At Fernandina, the jump in the semidiurnal tide amplitude in 1905 are shown in the two methods, which are not reported in existing publications. Consistent with the findings of Müller (2011), high temporal M_2 amplitude variability found with the two methods is coherent in the Gulf of Maine (Eastport, Portland and Boston). Strong variability is also shown in the South Atlantic Bight (Charleston, Fernandina and Pulaski). The stations at the Mid-Atlantic Bight region demonstrate relatively lower temporal M_2 amplitude variability, with the M_2 amplitude decreasing in the Chesapeake Bay (Chesapeake Bay Bridge Tunnel, Kiptopeke and Sewells Point) and in the Delaware Bay (Lewes) from HA. A phase lag of ~ 1 year between the EMD and HA analyses is shown at Kiptopeke. The correlation increases from 0.63 to 0.90 when the phase lag is adjusted in the time series. The cause of this lag is not clear, but since the record at this site is relatively short, the accuracy of the EMD calculations is less than that in stations with longer records.

The largest discrepancy between the EMD and HA is seen in Baltimore, so further investigation is conducted. Since it is evident in Fig. 2 that the EMD mode-1 captures more than the M_2 alone, the variations in the (four) main semidiurnal tidal constituents are calculated by HA for Baltimore and shown in Fig. 4. Showing the EMD results on a different y-axis than HA (Fig. 4a) indicates that the shift in the amplitude of the M_2 tide around 1970 is in fact very similar in both methods (though the magnitude of the shift is different). The correlation between the HA and EMD derived amplitude variations increase to

0.9 if only the data after 1970 were considered. It is also interesting to note that N_2 shows a similar increase in amplitude in recent years as M_2 does, but S_2 on the other hand shows a decrease in amplitude in recent years (and K_2 shows no clear trend at all). It is not clear what caused this shift, but there is a change in tidal characteristics that is detected by the EMD analysis. The discrepancy between the EMD and HA results in Key West are also accommodated by a frequency changes in mode-1 around 1970 (not shown); such non-stationary changes cannot be obtained from the HA analysis. It is thus reasonable to conclude that the EMD cannot calculate the exact magnitude of the semidiurnal tides as HA does, but it is a useful tool to detect changes.

To further investigate the discrepancy between EMD and HA at Baltimore and Key West, Fig. 5a and b show the changes of M_2 and EMD mode 1 when the time series for EMD analysis is separated into two sections, before and after the amplitude jump. In this test, the two methods agree with each other much better than the case when the EMD analyzed the entire record at once, demonstrating that a sudden change in the data is probably being amplified by the EMD analysis. This is an important point to know, as the usage of EMD is expanded to new fields.

4. Discussion and summary

The EMD has been widely used for various geophysical data analysis, but to our knowledge it has not been used before for studies of variations in characteristics of tides. The HA on the other hand is a widely used method to analyze tides and investigate potential changes in tidal properties (e.g., Mawdsley et al., 2015). This study is possibly the first test that tries to adopt the EMD technique to describe the semidiurnal tide amplitude variability using the hourly tide gauge records. The results show high consistency with that obtained from the HA method, but there are some exceptions because of the different nature of the two methods. The EMD is a non-stationary empirical method that has no assumptions about the expected period of tidal constituents, so if the sea level is dominated by the M_2 tides, as is the case in the U.S. East Coast, the highest frequency mode of the EMD represents to large extend the variability of M_2. However, other semidiurnal tides and non-tidal variability may also be captured by the EMD. It is encouraging and somewhat surprising how well the EMD agrees with the results of the standard HA analysis (in most cases). Because the EMD is applied at once to entire records it is a quick way to detect unusual sudden changes that may be the results of instrumental replacement/errors or man-made changes such as dredging. One should be cautious though, since the EMD may amplify sudden changes in data, as was the case for two locations (Baltimore and Key West).

At Wilmington, both HA and EMD analyses demonstrate similar significant increase in the M_2 amplitude due to increased channel depths (Familkhalili and Talke, 2016). Consistent with the study of Müller (2011), in the South Atlantic Bight, the M_2 tidal amplitude increased at Charleston until ~ 1980 and then remains flat (Ray, 2006). The other two tide gauges (Fort Pulaski and Fernandina) also show notable M_2 amplitude variability with a negative offset after 1980 with the removal of trend during 1930–1980, which might be associated with response to decadal variability in the Atlantic Ocean (Ezer, 2015).

The great advantage of HA over the EMD is the predictability for tidal phenomena based on the astronomical movement. Compared with HA, the advantage of the EMD is that it is more general and can systematically filter out oscillating modes with unknown and variable frequencies. Moreover, the EMD provides frequency information of storm surges and other sea level variations on different time scales from weekly to decadal, though here only the highest modes relating to the main tidal cycles where analyzed.

The difference between the EMD and HA derived M_2 amplitude evolution is dominated by the nodal cycle, which is captured by the EMD analysis, so it needs to be removed when studying long term changes in tidal amplitudes. The nodal cycle can significantly contribute to regional coastal changes (e.g., Gratiot et al., 2008) and impact coastal high tidal levels (Haigh et al., 2011). Accounting for global median amplitude of 2.2 cm nodal cycle is crucial to accurately estimate regional SLR. The EMD method demonstrates nodal cycle modulations (not shown) of ~ 2–3% (e.g., 1–6 cm) of semidiurnal tides amplitude at the selected tide gauges along the U.S east coast. The magnitude is consistent with findings based on equilibrium tide expectation (Fig. 1b of Haigh et al., 2011).

Since the extremely slow changes of the astronomical forcing, tides are usually thought of as stationary (Jay, 2009). In most cases, the changes are not fully understood and may be region-dependent (Woodworth, 2010), as the physical processes cause the tidal variations are complicated (Ray, 2006, 2009; Mawdsley et al., 2015; Ray and Foster, 2016). The responses of tide change (mainly in semidiurnal constituents M_2 and S_2) to future SLR are significant on the east coast of the US (Pickering et al., 2017). In the Gulf of Maine for example, some small changes in topography or water properties can cause significant changes in the large tides due to the high resonant state of the M_2 tide (Greenberg et al., 2012; Mawdsley et al., 2015). In the Chesapeake and Delaware Bays, both the vertical land motion and the changes of estuarine geometry and high sea level rise rate may be responsible to the observed M_2 amplitude decrease in the lower Chesapeake Bays (Lee et al., 2017), which agrees with the findings in Pickering et al. (2017) that allow coastal recession may amplifies the tidal response but become decrease in response of future SLR scenarios. The results here for the upper Chesapeake Bay (Baltimore) show an increase in the amplitude of M_2 and a decrease in S_2. Note however, that the largest change there in tidal characteristics is not gradual but a rapid change. The exact reasons caused the variations are still not clear.

The high frequency variations discussed here are not independent from long term variations in sea level along US east coast that may relate to variations in AMOC and the GS (e.g., Ezer, 2015; Ezer et al., 2013; Ezer et al., 2016; Han et al., 2018; Lorbacher et al., 2010; Yin and Goddard, 2013). For example, period of months to few years with higher than normal sea level due to weakening AMOC or low North Atlantic Oscillation index (Ezer and Atkinson, 2014; Ezer, 2015) can also be accompanied by interannual variations in tidal amplitudes. Variations in GS transport produce variations in sea level gradient across the entire GS length and this large-scale signal is then transmitted into the shelf by the generation of coastal-trapped waves (Ezer, 2016). However, the exact mechanism of how changes in offshore currents such as the GS and changes in wave field may affect the tidal variability over the different regions, will require further research. The EMD seems to be a useful tool to study those non-stationary changes, but it always recommended to compare it with other analysis methods as done here.

In summary, this study is a proof of concept demonstration of a new analysis tool that, together with well-established tools like HA, can provide additional tidal information and detect time-dependent and space-dependent changes in tidal characteristics, due to natural variability, man-made coastal modifications and global climate change.

Acknowledgement

This study was supported by Old Dominion University's Climate Change and Sea Level Rise Initiative (CCSLRI), the National Key Project of Research and Development Plan of China (Grant no. 2016YFC1401905), National Natural Science Foundation of China (Grant no. 41576168), and the Fundamental Research Funds for the Central Universities (Grant no. 2015B15914). We are thankful to the reviewers and editor for their constructive comments and suggestions. The hourly tide gauge data is available from http://opendap.co-ops.nos.noaa.gov/dods/IOOS/.

Appendix A

(See Figs. A1–A3).

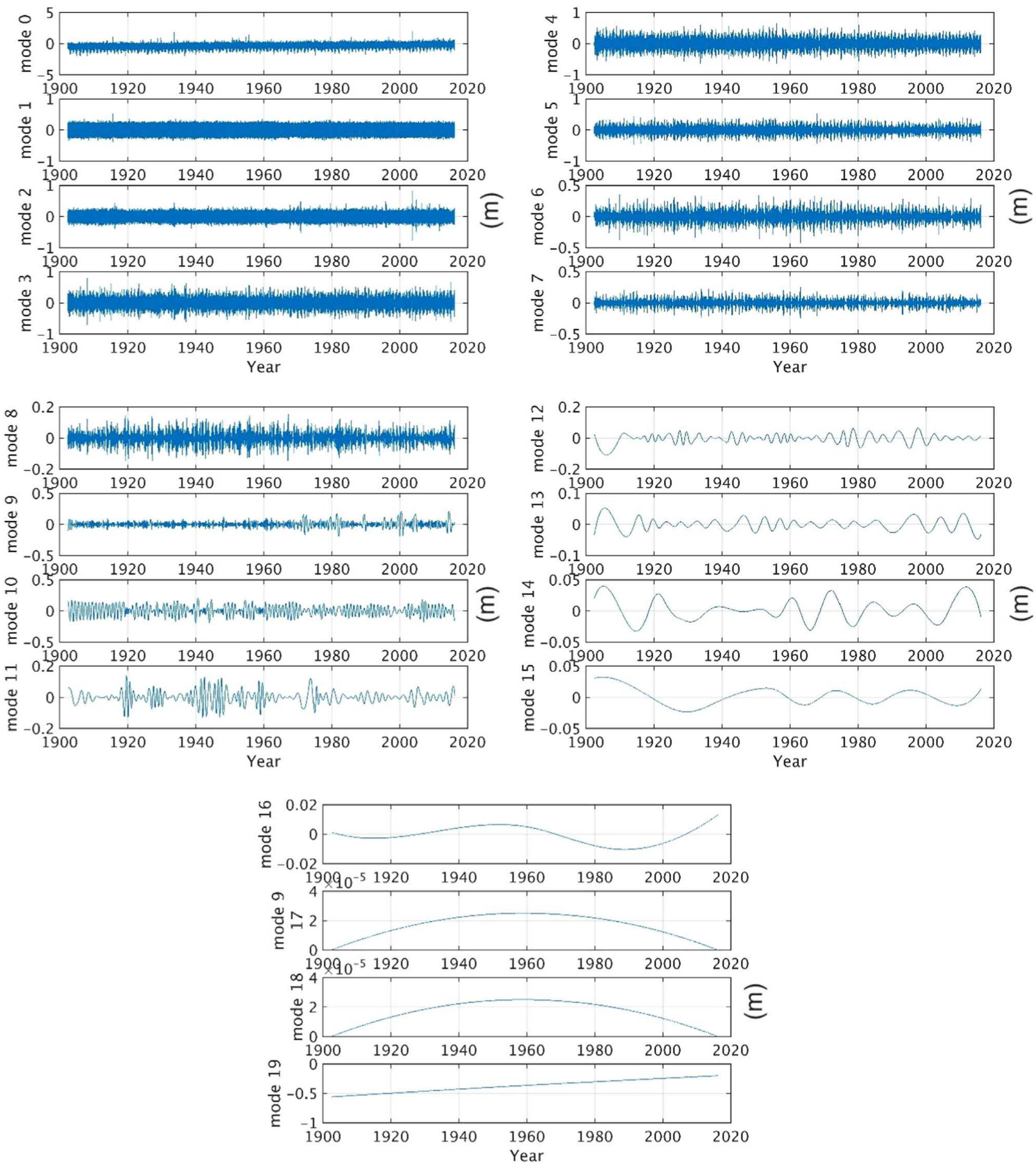

Fig. A1. The EMD analysis (m) for the Baltimore sea level data (mode 1–19, mode 0 denote original tide gauge records).

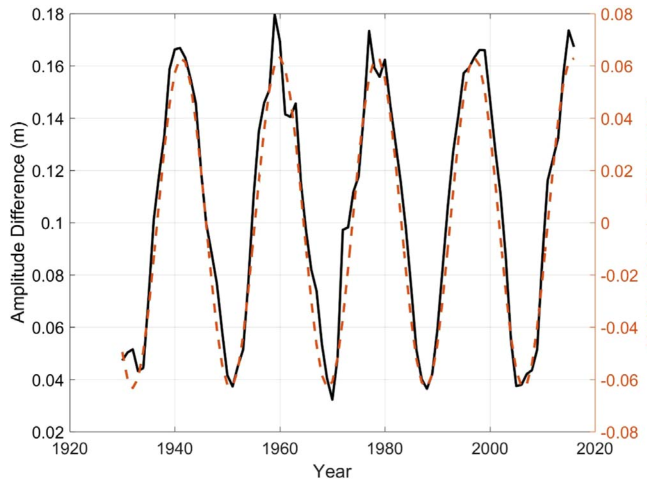

Fig. A2. The difference (black curve, m) between the sea level variation magnitude and M_2 amplitude calculated with EMD analysis (mode 1) and HA. The dashed line is the nodal cycle estimated from EMD (mode 1) sea level variation (m) using Eq. (2).

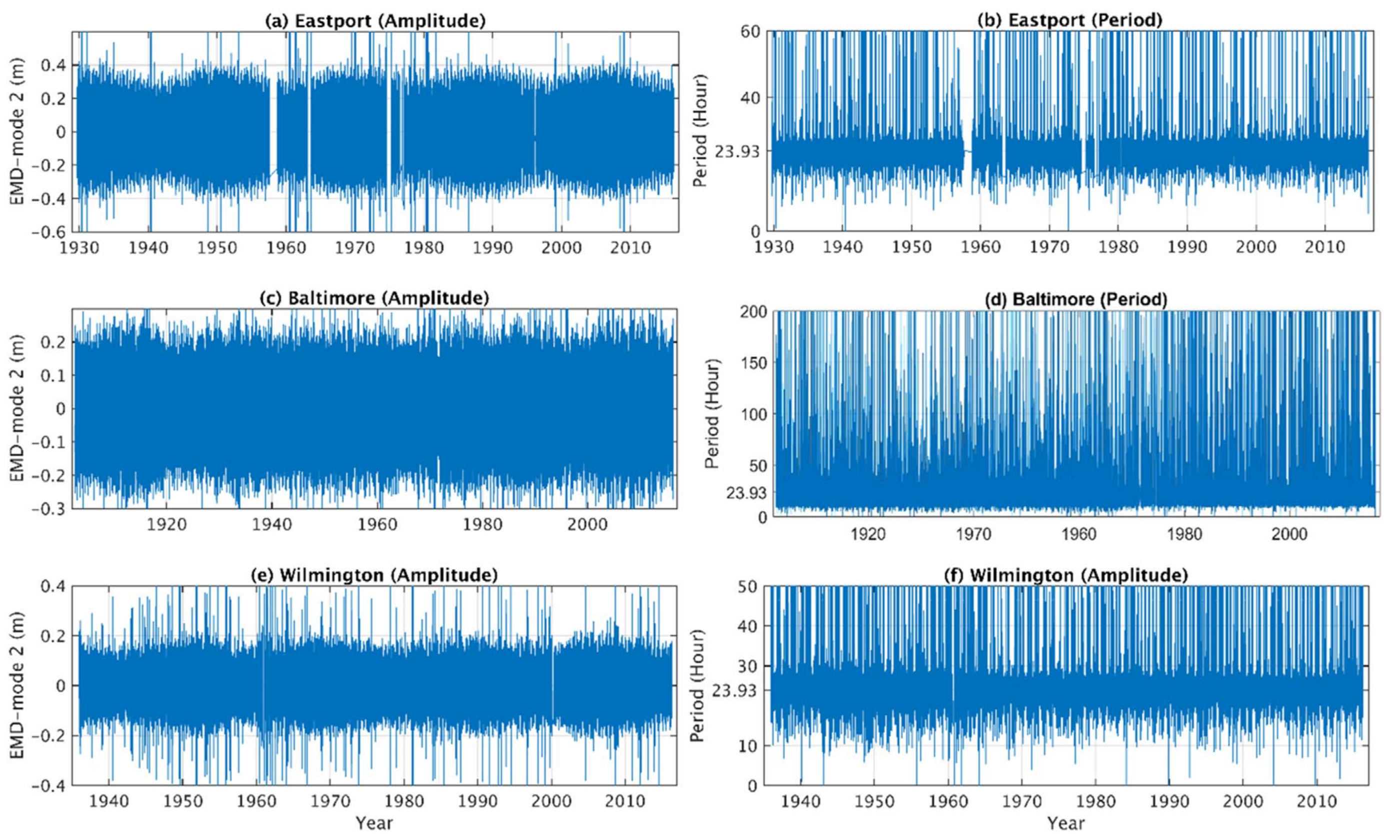

Fig. A3. Similar to Fig. 2, but for EMD mode-2.

References

Atkinson, L.P., Ezer, T., Smith, E., 2012. Sea level rise and flooding risk in Virginia. Sea Grant Law Policy J. 5, 3.

Bell, C., Vassie, J.M., Woodworth, P.L., 1996. The Tidal Analysis Software Kit (TASK Package). TASK-2000 Version Dated December 1998. Available from 〈www.psmsl.org〉.

Bonaduce, A., Pinardi, N., Oddo, P., Spada, G., Larnicol, G., 2016. Sea-level variability in the Mediterranean Sea from altimetry and tide gauges. Clim. Dyn. 1–16.

Cheng, Y., Ezer, T., Hamlington, B.D., 2016. Sea level acceleration in the China seas. Water 8, 293.

Church, J.A., White, N.J., 2011. Sea-level rise from the late 19th to the early 21st century. Surv. Geophys. 32, 585–602.

Codiga, D.L., 2011. Unified Tidal Analysis and Prediction Using the UTide Matlab Functions, Technical Report 2011-01. Graduate School of Oceanography, University of Rhode Island, Narragansett, RI, pp. 59. ftp://www.po.gso.uri.edu/pub/downloads/codiga/pubs/2011Codiga-UTide-Report.pdf.

Ezer, T., 2013. Sea level rise, spatially uneven and temporally unsteady: why the US East Coast, the global tide gauge record, and the global altimeter data show different trends. Geophys. Res. Lett. 40, 5439–5444. http://dx.doi.org/10.1002/2013GL057952.

Ezer, T., 2015. Detecting changes in the transport of the Gulf Stream and the Atlantic overturning circulation from coastal sea level data: the extreme decline in 2009–2010 and estimated variations for 1935–2012. Glob. Planet. Change 129, 23–36. http://dx.doi.org/10.1016/j.gloplacha.2015.03.002.

Ezer, T., 2016. Can the Gulf Stream induce coherent short-term fluctuations in sea level along the US East Coast? A modeling study. Ocean Dyn. 66, 207–220. http://dx.doi.

org/10.1007/s10236-016-0928-0.
Ezer, T., Atkinson, L.P., 2014. Accelerated flooding along the US East Coast: on the impact of sea-level rise, tides, storms, the Gulf Stream, and the North Atlantic oscillations. Earth's. Future 2, 362–382. http://dx.doi.org/10.1002/2014EF000252.
Ezer, T., Atkinson, L.P., Corlett, W.B., Blanco, J.L., 2013. Gulf Stream's induced sea level rise and variability along the US mid-Atlantic coast. J. Geophys. Res.: Oceans 118, 685–697. http://dx.doi.org/10.1002/jgrc.20091.
Ezer, T., Corlett, W.B., 2012. Is sea level rise accelerating in the Chesapeake Bay? A demonstration of a novel new approach for analyzing sea level data. Geophys. Res. Lett. 39, L19605. http://dx.doi.org/10.1029/2012GL053435.
Ezer, T., Haigh, I.D., Woodworth, P.L., 2016. Nonlinear Sea-Level Trends and Long-Term Variability on Western European Coasts. J. Coast. Res. 320, 744–755. http://dx.doi.org/10.2112/JCOASTRES-D-15-00165.1.
Familkhalili, R., Talke, S., 2016. The effect of channel deepening on tides and storm surge: a case study of Wilmington, NC. Geophys. Res. Lett. 43, 9138–9147.
Flandrin, P., Rilling, G., Goncalves, P., 2004. Empirical mode decomposition as a filter bank. IEEE Signal Process. Lett. 11, 112–114.
Flick, R.E., Murray, J.F., Ewing, L.C., 2003. Trends in United States tidal datum statistics and tide range. J. Waterw. Port. Coast. Ocean Eng. 129, 155–164.
Foreman, M., 1977. Manual of Tidal Heights Analysis and Prediction. Institute of Ocean Sciences, Victoria, British Columbia (Pacific Marine Sciences Report 77-10).
Gratiot, N., Anthony, E.J., Gardel, A., Gaucherel, C., Proisy, C., Wells, J., 2008. Significant contribution of the 18.6 year tidal cycle to regional coastal changes. Nat. Geosci. 1, 169–172.
Greenberg, D.A., Blanchard, W., Smith, B., Barrow, E., 2012. Climate change, mean sea level and high tides in the Bay of Fundy. Atmos. Ocean 50, 261–276.
Haigh, I.D., Eliot, M., Pattiaratchi, C., 2011. Global influences of the 18.61 year nodal cycle and 8.85 year cycle of lunar perigee on high tidal levels. J. Geophys. Res.: Oceans 116, C06025. http://dx.doi.org/10.1029/2010JC006645.
Han, W., Meehl, G.A., Stammer, D., Hu, A., Hamlington, B., Kenigson, J., Palanisamy, H., Thompson, P., 2018. Spatial patterns of sea level variability associated with natural internal climate modes. Surv. Geophys. 38 (1), 217–250.
Houston, J.R., Dean, R.G., 2011. Sea-level acceleration based on US tide gauges and extensions of previous global-gauge analyses. J. Coast. Res. 27, 409–417.
Huang, N.E., Shen, Z., Long, S.R., Wu, M.C., Shih, H.H., Zheng, Q., Yen, N.-C., Tung, C.C., Liu, H.H., 1998. The empirical mode decomposition and the Hilbert spectrum for nonlinear and non-stationary time series analysis. Proc. R. Soc. Lond. A: Math. Phys. Eng. Sci. R. Soc. 903–995.
Huang, N.E., Wu, Z., 2008. A review on Hilbert-Huang transform: method and its applications to geophysical studies. Rev. Geophys. 46, RG2006. http://dx.doi.org/10.1029/2007RG000228.
Huang, N.E., Wu, M.L., Long, S.R., Shen, S.S., Qu, W., Gloersen, P., Fan, K.L., 2003. A confidence limit for the empirical mode decomposition and Hilbert spectral analysis. Proc. R. Soc. Lond. A 459 (2037), 2317–2345.
Jay, D.A., 2009. Evolution of tidal amplitudes in the eastern Pacific Ocean. Geophys. Res. Lett. 36, L04603. http://dx.doi.org/10.1029/2008GL036185.
Kopp, R.E., 2013. Does the mid-Atlantic United States sea level acceleration hot spot reflect ocean dynamic variability? Geophys. Res. Lett. 40, 3981–3985.
Lee, S.B., Li, M., Zhang, F., 2017. Impact of sea level rise on tidal range in Chesapeake and Delaware Bays. J. Geophys. Res.: Oceans 122. http://dx.doi.org/10.1002/2016JC012597.
Li, F., Jo, Y.-H., Yan, X.-H., Liu, W.T., 2016. Climate signals in the mid to high latitude North Atlantic from altimeter observations. J. Clim. 29 (13), 4905–4925.
Li, Y., Zhang, H., Tang, C., Zou, T., Jiang, D., 2016. Influence of Rising Sea Level on Tidal Dynamics in the Bohai Sea. J. Coast. Res. 74, 22–31.
Lorbacher, K., Dengg, J., Böning, C.W., Biastoch, A., 2010. Regional patterns of sea level change related to interannual variability and multidecadal trends in the Atlantic meridional overturning circulation*. J. Clim. 23, 4243–4254.
Mawdsley, R.J., Haigh, I.D., Wells, N.C., 2015. Global secular changes in different tidal high water, low water and range levels. Earth's. Future 3, 66–81.
Müller, M., 2011. Rapid change in semi-diurnal tides in the North Atlantic since 1980. Geophys. Res. Lett. 38, L11602. http://dx.doi.org/10.1029/2011GL047312.
Pawlowicz, R., Beardsley, B., Lentz, S., 2002. Classical tidal harmonic analysis including error estimates in MATLAB using T_TIDE. Comput. Geosci. 28, 929–937.
Pelling, H.E., Green, J.M., Ward, S.L., 2013. Modelling tides and sea-level rise: to flood or not to flood. Ocean Model. 63, 21–29.
Pickering, M.D., Horsburgh, K.J., Blundell, J.R., Hirschi, J.J.M., Nicholls, R.J., Verlaan, M., Wells, N.C., 2017. The impact of future sea-level rise on the global tides. Cont. Shelf Res. http://dx.doi.org/10.1016/j.csr.2017.02.004.
Ray, R.D., 2006. Secular changes of the M2 tide in the Gulf of Maine. Cont. Shelf Res. 26, 422–427.
Ray, R.D., 2009. Secular changes in the solar semidiurnal tide of the western North Atlantic Ocean. Geophys. Res. Lett. 36, L19601. http://dx.doi.org/10.1029/2009GL040217.
Ray, R.D., Foster, G., 2016. Future nuisance flooding at Boston caused by astronomical tides alone. Earth's. Future. http://dx.doi.org/10.1002/2016EF000423.
Sallenger, A.H., Doran, K.S., Howd, P.A., 2012. Hotspot of accelerated sea-level rise on the Atlantic coast of North America. Nat. Clim. Change 2, 884–888.
Sha, J., Jo, Y.H., Yan, X.H., Liu, W., 2015. The modulation of the seasonal crossshelf sea level variation by the cold pool in the middle Atlantic Bight. J. Geophys. Res.: Oceans 120, 7182–7194.
Sweet, W.V., Park, J., 2014. From the extreme to the mean: acceleration and tipping points of coastal inundation from sea level rise. Earth's. Future 2, 579–600.
Tebaldi, C., Strauss, B.H., Zervas, C.E., 2012. Modelling sea level rise impacts on storm surges along US coasts. Environ. Res. Lett. 7, 014032.
Wahl, T., Calafat, F.M., Luther, M.E., 2014. Rapid changes in the seasonal sea level cycle along the US Gulf coast from the late 20th century. Geophys. Res. Lett. 41, 491–498.
Wahl, T., Chambers, D.P., 2016. Climate controls multidecadal variability in US extreme sea level records. J. Geophys. Res.: Oceans 121, 1274–1290. http://dx.doi.org/10.1002/2015JC011057.
Wdowinski, S., Bray, R., Kirtman, B.P., Wu, Z., 2016. Increasing flooding hazard in coastal communities due to rising sea level: case study of Miami Beach, Florida. Ocean Coast. Manag. 126, 1–8.
Woodworth, P., 2010. A survey of recent changes in the main components of the ocean tide. Cont. Shelf Res. 30, 1680–1691.
Woodworth, P., 2011. A note on the nodal tide in sea level records. J. Coast. Res. 28, 316–323. http://dx.doi.org/10.2112/jcoastres-d-11a-00023.1.
Wu, Z., Huang, N.E., 2009. Ensemble empirical mode decomposition: a noise-assisted data analysis method. Adv. Adapt. Data Anal. 1, 1–41.
Yin, J., Goddard, P.B., 2013. Oceanic control of sea level rise patterns along the East Coast of the United States. Geophys. Res. Lett. 40, 5514–5520.
Zhang, H., Sheng, J., 2013. Estimation of extreme sea levels over the eastern continental shelf of North America. J. Geophys. Res.: Oceans 118, 6253–6273.
Zhang, K., 2011. Analysis of non-linear inundation from sea-level rise using LIDAR data: a case study for South Florida. Clim. Change 106, 537–565.